İSTANBUL TECHNICAL UNIVERSITY ★ INSTITUTE OF SCIENCE AND TECHNOLOGY

ACCRETION IN THE SPIN-DOWN REGIME OF ACCRETING MILLISECOND X-RAY PULSARS

M.Sc. Thesis by
Erlin KUTLU

Department : **Physics Engineering**
Programme : **Physics Engineering**

JUNE 2011

İSTANBUL TECHNICAL UNIVERSITY ★ INSTITUTE OF SCIENCE AND TECHNOLOGY

ACCRETION IN THE SPIN-DOWN REGIME OF ACCRETING MILLISECOND X-RAY PULSARS

M.Sc. Thesis by
Erlin KUTLU
(509021111)

Date of Submission : **06 May 2011**
Date of Examination : **07 June 2011**

Supervisor (Chairman) : **Assoc.Prof.Dr. K.Yavuz EKŞİ (ITU)**
Members of the Examining Committee : **Prof.Dr. A.Togo GİZ (ITU)**
Assoc.Prof.Dr. M.Hakan ERKUT (IKU)

JUNE 2011

İSTANBUL TEKNİK ÜNİVERSİTESİ ★ FEN BİLİMLERİ ENSTİTÜSÜ

MİLİSANİYE X-IŞINI PULSARLARININ YAVAŞLAMA EVRESİNDE KÜTLE AKTARIMI

YÜKSEK LİSANS TEZİ

Erlin KUTLU
(509021111)

Tezin Enstitüye Verildiği Tarih : 06 Mayıs 2011
Tezin Savunulduğu Tarih : 07 Haziran 2011

Tez Danışmanı : Doç.Dr. K.Yavuz EKŞİ (İTÜ)
Diğer Jüri Üyeleri : Prof.Dr. A.Togo GİZ (İTÜ)
Doç.Dr. M.Hakan ERKUT (İKÜ)

HAZİRAN 2011

FOREWORD

I would like to express my deep appreciation and thanks to my advisor Assoc. Prof. Kazım Yavuz EKŞİ, for his guidance, patience, encouragement, and support from beginning to final level of completion of my thesis.

I would also like to thank my family and my friends, they always supported me and encouraged me during the completion of my thesis.

And I want to thank Istanbul Technical University Physics Engineering Department.

June 2011

Erlin KUTLU
B.S.

TABLE OF CONTENTS

Page

ABBREVIATIONS

ADAF	:	Advection Dominated Accretion Flow
AMXP	:	Accreting Millisecond X-ray Pulsar
HMXB	:	High Mass X-ray Binary
kHz QPO	:	Kilo Hertz Quasi Periodic Oscillations
LMXB	:	Low Mass X-ray Binary
NS	:	Neutron Star
NS LMXB	:	Neutron Star Low Mass X-ray Binary
QPO	:	Quasi Periodic Oscillations
RPP	:	Rotationally Powered Pulsar

LIST OF FIGURES

LIST OF SYMBOLS

a	:	Binary separation
B	:	Magnetic field
c	:	Speed of light in vacuum
d	:	Distance of object
f	:	Fraction of inflowing mass that can accrete
$F_{\rm X}$	:	X-ray Flux
G	:	Gravitational constant
J_*	:	Stellar angular momentum
$\dot{J}$	:	Angular momentum flux
L	:	Accretion Luminosity
$L_{\rm c}$	:	Critical luminosity
$L_{\rm d}{\it isk}$	:	Disk luminosity
$M_\odot$	:	Solar mass
M_*	:	Neutron star mass
M_1	:	Mass of the primary star
M_2	:	Mass of the secondary star
$\dot{M}$	:	Mass inflow rate in the disk
N_0	:	Accretion torque
P	:	Rotational Period of the Neutron Star
$P_{\rm orb}$	:	Orbital Period
$P_{\rm mag}$	:	Magnetic pressure
$P_{\rm ram}$	:	Ram pressure
q	:	Mass ratio
$R_{\rm A}$	:	Alfvén radius
$R_{\rm co}$	:	Corotation radius
$R_{\rm i}n$	:	Inner radius of the disk
R_*	:	Neutron star radius
$v_{\rm ff}$	:	Free fall velocity
V_R	:	Radial velocity
α	:	Inclination angle
α_{SS}	:	Viscosity parameter
η	:	Compactness parameter
μ	:	Magnetic moment
ν	:	Kinematic Viscosity
ω_*	:	Fastness parameter
Ω_*	:	Angular velocity of the star
$\Phi_{\rm R}$	:	Roche potential
σ	:	Stefan-Boltzmann constant
Σ	:	Surface mass density

ACCRETION IN THE SPIN-DOWN REGIME OF ACCRETING MILLISECOND X-RAY PULSARS

SUMMARY

Accreting millisecond X-ray pulsars (AMXP), the first of which is discovered in 1998, form a sub-class of low mass X-ray binaries. Up to date thirteen AMXPs have been discovered. AMXPs are neutron stars accreting from a surrounding disk. The matter in the disk comes from the low mass companion of the neutron star through Roche Lobe overflow.

Accreting millisecond X-ray pulsars show outbursts originating from an instability in the disk. The lightcurves at the outburst stage show a rapid decay episode following a slow decay episode. The rapid decay episode had been associated with transition to the propeller stage. If the disk is thin no matter can accrete onto the neutron star in this stage and the luminosity is expected to drop more abruptly than observed. If the disk is thick matter can accrete onto the neutron star from locations away from the disk plane. Explanation of the rapid decay stage with transition to the propeller stage requires the inner disk to be thick.

In this thesis the fraction of the inflowing matter that can accrete onto the neutron star, depending on the fastness parameter and the inclination angle between the magnetosphere and the disk, is calculated. The model is then used to model the lightcurve of the millisecond X-ray pulsar SAX J1808.4-3658. It is shown that the fraction of mass that can accrete is doubly-valued for small inclination angles. This allows the system to have different luminosities at a single fastness parameter. According to this result, transitions from the full accretion to the propeller regime and from propeller to the accretion regime will occur at different luminosities, if the inclination angle is small. According to the conventional propeller models such transitions should take place at a single luminosity in each system. Such hysteresis behavior had already been observed from the millisecond X-ray pulsar, Aql X-1. The theoretical framework proposed in this thesis predicts that the inclination angle in Aql X-1 is small.

MİLİSANİYE X-IŞINI PULSARLARININ YAVAŞLAMA EVRESİNDE KÜTLE AKTARIMI

ÖZET

İlki 1998'de keşfedilen milisaniye X-ışını pulsarları küçük kütleli X-ışını çiftlerinin bir alt sınıfını oluşturur. Günümüze dek on üç milisaniye X-ışını pulsarı bulunmuştur. Milisaniye X-ışını pulsarları etrafındaki diskten kütle aktarımı yapan nötron yıldızlarıdır. Diskteki madde nötron yıldızına eşlik eden küçük kütleli yıldızdan Roche lobe taşması yoluyla gelir.

Milisaniye X-ışını pulsarları kütle aktarım diskinin kararsızlığından kaynaklanan geçici parlama evresi gösterirler. Parlama dönemindeki ışık eğrilerinde ışıma gücünün yavaş azaldığı evreyi takip eden bir hızlı azalma evresi görülür. Hızlı azalma evresi sistemin "pervane" aşamasına geçmesi ile ilişkilendirilmiştir. Ancak diskin iç kısımları ince ise bu evrede yıldız üzerine düşen kütlenin sıfır olması, dolayısı ile ışımanın daha da keskin biçimde azalması beklenir. Eğer disk kalın ise disk düzleminden uzaktaki bölgeden yıldız üzerine kütle aktarımı gerçekleşebilir. Hızlı azalma evresinin "pervane" aşamasına geçişle açıklanması diskin iç kısımlarının kalın olmasını gerektirir.

Bu tezde yıldızın dönme parametresine ve manyetosfer ile disk arasındaki eğim açısına bağlı olarak diskte içeriye taşınan maddenin ne kadarlık bir kesrinin nötron yıldızı üzerine düşebileceği hesaplanmıştır. Bu model daha sonra SAX J1808.4-3658 adlı milisaniye X-ışını pulsarının ışık eğrisinin modellenmesinde kullanılmıştır. Küçük eğim açıları için düşen madde miktarının aynı dönme parametresinde iki-değerli olabileceği gösterilmiştir. Bu durum kaynağın aynı dönme parametresinde iki farklı ışıma gücüne sahip olabilmesine izin verir. Bu sonuca göre, düşük eğim açısına sahip sistemlerde, tam kütle aktarımı aşamasından pervane aşamasına geçiş ve pervane aşamasından tam kütle aktarımı aşamasına geçiş farklı ışıma gücünde gerçekleşir. Kullanılagelmiş pervane modellerinde bu geçişler her sistemde tek bir ışıma gücünde gerçekleşmek durumundadır. Bu türden bir histerezis davranışı Aql X-1 adlı milisaniye X-ışını pulsarında gözlemlenmiştir. Bu tezde önerilen kuramsal çerçeve Aql X-1 sisteminde eğim açısının küçük olduğu öndeyisinde bulunmaktadır.

1. INTRODUCTION

In this thesis I worked on the accretion in the spin down regime of accreting millisecond X-ray pulsars (AMXPs). The purpose of my thesis is to explain the rapid decay stage in the lightcurves of AMXPs as partial accretion in the spin down regime.

Low mass X-ray binary (LMXB) systems consist of a neutron star (NS) and a mass donor companion. LMXBs are old binary systems with a low mass companion. The AMXPs form a subset of NS LMXBs. They are all transient systems and are discovered in their outburst stages. Discovery of the first AMXP in 1998 [3] was very important in supporting the recycling hypothesis [4] suggesting that millisecond radio pulsars descend from LMXBs. Today there are 13 known AMXPs. The general properties of NSs and their astrophysical manifestations are discussed in Chapter 2.

In LMXBs the accretion disks form through mass transfer of material from the companion via Roche lobe overflow. Accretion disk structure and the accretion processes are reviewed in Chapter 3.

In Chapter 4 I discuss the so called "propeller effect" [5] and the possibility of accretion during this stage [6, 7]. I derive an estimate of the fraction of the inflowing mass in the disk that can accrete onto the NS in the spin down regime, depending on the fastness parameter and the inclination angle between the rotational and the magnetic axis of the NS. In this original part of the thesis, I find that, for small inclination angles, transitions between the accretion and propeller regimes can show hysteresis like behavior in the sense that transition from accretion to the propeller regime can occur at a different luminosity than transition from the propeller back to the accretion regime. In conventional propeller models such transitions should take place at a single luminosity for each system. Aql X-1 shows sudden drop in luminosity being reminiscent of transition to the propeller stage. The system also shows an hysteresis like effect, for the transition back to the accretion stage does not occur at the same luminosity. This had been used to argue against the presence of propeller transition

in this system [8] relying on the conventional propeller models. The theoretical framework presented in this thesis which has two different critical luminosities for forward and backward transitions between accretion and propeller regimes obviates such arguments that discard, relying on the presence of the hysteresis effect, the transition to the propeller regime as an explanation of the luminosity drop.

In Chapter 4 I model the lightcurve of SAX J1808.4-3658, the first AMXP discovered, from the rise, peak, slow decay to the rapid decay stage. This shows a continuous lightcurve and the inclination angle is accordingly large, requirement of the model presented in this thesis. In the case of Aql X-1, the lightcurve shows a discontinuous drop in luminosity accompanied by hysteresis effect in transition back, which can be addressed in my model with small inclination angles. A prediction of my model is indeed that systems which show discontinuous drop in luminosity in transition to the propeller stage must also show the hysteresis effect.

In the last chapter I discuss my results, the limitations of the model and possible directions for improving the model in the future.

2. GENERAL PROPERTIES AND MANIFESTATIONS OF NEUTRON STARS

In this Chapter I review the general properties and manifestations of neutron stars (NS).

2.1 Neutron Stars

Neutron stars are compact objects with radius $R \simeq 10$ km and mass $M \simeq 1.5 M_\odot$. The average density is then

$$\bar{\rho} = \frac{M}{\frac{4}{3}\pi R^3} = 4.75 \times 10^{15}\,\mathrm{g\,cm^{-3}} \left(\frac{M}{M_\odot}\right) \left(\frac{R}{10\,\mathrm{km}}\right)^{-3}. \tag{2.1}$$

Their central densities might reach 10^{16} g cm^{-3} exceeding that of nuclear densities. The equation of state at such densities is not yet probed by experiments on the Earth. Neutron stars are supported against their own gravitation by the degeneracy pressure of interacting neutrons; at such densities the repulsive nature of the interaction assists the degeneracy pressure of the neutrons.

The compactness parameter of a NS is

$$\eta \equiv \frac{GM}{c^2 R} = 0.15 \left(\frac{M}{M_\odot}\right) \left(\frac{R}{10\,\mathrm{km}}\right)^{-1} \tag{2.2}$$

where G is the gravitational constant and c is the speed of light. As this dimensionless parameter is close to unity, general relativity is necessary for describing NSs adequately. The structure of NSs in hydrostatic equilibrium are described by Tolman-Oppenheimer-Volkoff equations [9, 10]:

$$\frac{dm}{dr} = 4\pi r^2 \rho \tag{2.3}$$

where $m = m(r)$ is the gravitational mass inside the radius r and

$$\frac{dP}{dr} = -\frac{Gm\rho}{r^2} \left(1 + \frac{P}{\rho c^2}\right) \left(1 + \frac{4\pi r^3 P}{mc^2}\right) \left(1 - \frac{2Gm}{rc^2}\right)^{-1} \tag{2.4}$$

where P is the pressure. These equations must be supported by an equation of state, $P = P(\rho)$, appropriate for densities prevailing in NSs.

Neutron stars can have extremely high magnetic fields: $B \sim 10^{12}$ G in the case of young rotationally powered pulsars (RPPs) [11] and high mass X-ray binaries (HMXBs) [12], $B \sim 10^{8}$ G in the case of millisecond RPP [13] and low mass X-ray binaries (LMXBs) [4], and $B \sim 10^{15}$ G in the case of magnetars [14].

Neutron stars can rotate very rapidly with periods of milliseconds in the case of millisecond RPP and LMXBs. The first discovered millisecond radio pulsar PSR 1937+21 [15] has a spin period $P = 1.5578$ ms i.e. rotates about its axis 642 times per second.

Compact objects are born when the nuclear life of a star ends. The progenitors of NSs are the high-mass stars with $M \gtrsim 8M_{\odot}$. At the end of its nuclear life, the core of the star collapses to form the NS and this produces a supernova explosion during which all layers surrounding the stellar core are expelled. High mass stars are born at the galactic plane where star forming regions exist. As high mass stars live short and do not have time to leave the galactic plane, most of the young NSs are also near the galactic plane.Some NSs are in globular clusters which are old systems out of the galactic plane. These are usually members of LMXB systems or millisecond RPPs.

2.2 History of Neutron Stars

In 1932 Chadwick discovered neutron. Soon after this discovery, in 1934, Baade and Zwicky [16] suggested that a neutron star existed at the center of the Crab nebula and conjectured that NSs form in supernova explosions.

The structure of NSs was calculated by Oppenheimer-Volkoff in 1939 [10] assuming the equation of state to be that of an ideal degenerate neutron gas. They have neglected the interactions between the nucleons and found the maximum mass of the NS to be $0.7M_{\odot}$. As this mass is less than the Chandrasekhar's limit $M_{\rm Ch} = 1.4M_{\odot}$ for the maximum mass of white dwarfs, it was thought that stellar evolution would not produce NSs and they were disregarded until 1960's.

RPPs were discovered by Jocelyn Bell and Anthony Hewish in 1967 as radio pulsars [17]; Bell was a Phd student at Cambridge University working under the supervision of Hewish. Anthony Hewish won the Nobel Prize in 1974 due to his contribution to the discovery of radio pulsars.

The discovery of radio pulsars rekindled interest to NSs. X-ray pulsars like Sco X-1 was discovered by Giacconi et al.(1971) [18]. Giacconi received the Nobel prize in 2003 for his contributions to X-ray astronomy.

The first millisecond RPP were discovered in 1982 [15]. Simultaneously with this discovery the so called recycling hypothesis which suggests that millisecond RPP descend from NSs in LMXBs was proposed [4, 19]. Accreting millisecond X-ray pulsars (AMXPs) were discovered [3] in 1998 confirming the recycling hypothesis.

2.3 Manifestations of Neutron Stars

Thermal luminosity of a spherical object radiating as a black body is

$$L = 4\pi R^2 \sigma T^4 \tag{2.5}$$

where σ is Stefan-Boltzmann constant and T is the temperature. As their surface area is too small, the thermal luminosity of a NS will be very low compared to that of a main sequence star for a given temperature. For a typical NS radius Equation (**2.5**) gives, for $T \sim 10^6$ K, an X-ray luminosity of $L \sim 10^{33}$ erg s^{-1}. Because the thermal luminosity of a neutron star is low, only a few nearby cooling neutron stars are discovered up to date and indeed the first neutron stars were discovered by other means, as (rotationally powered) radio pulsars and (gravitationally powered) X-ray pulsars. These manifestations are shortly reviewed below.

2.3.1 Rotationally powered pulsars

RPPs are rapidly rotating NSs with strong magnetic fields. They radiate at the expense of their rotational energy. The rotational energy of the NS is converted to radiation via the magnetic dipole radiation mechanism [20–22].

2.3.2 Gravitationally powered neutron stars

Gravitationally powered NSs were discovered in 1971 by Giacconi et al. [18] as X-ray pulsars. They are rotating, strongly magnetized ($B \sim 10^9 - 10^{12}$ G) NSs accreting gas from a stellar companion in a binary system. The gravitational energy of the accreting material is released as X-ray and γ-ray radiation at the rate

$$L = \frac{GM\dot{M}}{R} \simeq 2 \times 10^{36} \text{ erg s}^{-1} \left(\frac{M}{1.4M_\odot}\right) \left(\frac{R}{10 \text{ km}}\right)^{-1} \left(\frac{\dot{M}}{10^{16} \text{ g s}^{-1}}\right) \tag{2.6}$$

where $\dot{M}$ is the mass accretion rate onto the surface of the NS.

If the magnetic dipole field of the NS is sufficiently high, the inflowing plasma is channeled to the magnetic polar caps modulating the radiation at the spin frequency if the magnetic dipole and rotation axes of the neutron star are not aligned. These polar caps are then rotating hot spots which are the sources of the pulsed emission. The periods of X-ray pulsars can be as short as milliseconds or can be more than several minutes.

2.3.3 Magnetically powered pulsars: magnetars

Magnetars are extremely magnetized ($B \sim 10^{15}$ G) NSs. Such magnetic fields are beyond the quantum critical limit

$$B_{\rm c} = \frac{m_e c^3}{e\hbar} = 4.4 \times 10^{13}\,{\rm G} \qquad (\mathbf{2.7})$$

at which the electron cyclotron energy, $\hbar\omega_c$, is equal to the rest mass energy $m_e c^2$. Their slow rotation period is clustered in the range of 5 to 12 seconds.

The observational manifestations of magnetars are soft gamma repeaters, and anomalous X-ray pulsars [14]. Another idea suggests that the persistent X-ray emission of these objects is powered by accretion from a fallback disk [23,24] while their super-Eddington bursts are powered by super-critical fields in higher multipoles [25,26]. The detection of optical and infrared emission with a disk-like spectrum [27] and upper limit on the dipole field of a magnetar [28] strongly supports this thesis [29].

2.4 X-Ray Binaries

Most of the stars are in binary systems where two stars rotate about the common center of mass. In the X-ray binary systems the primary star is a neutron star or a black hole accreting matter from the companion (secondary). X-ray binaries are divided into subclasses, according to the mass of the secondary star, as low mass X-ray binaries (LMXBs) and high mass X-ray binaries(HMXBs).

2.4.1 Low-mass x-ray binaries

LMXBs are usually very old systems in which the companion star is of low mass ($\leq 1 M_\odot$) and accretion is driven by Roche lobe overflow (see Chapter 3). The accreting

object can be a neutron star or a black hole. LMXBs are observed in the disk, bulge and globular cluster in the Milky Way [30].

If the accreting object is a NS and has sufficiently high magnetic fields such that the disk is disrupted at a distance away from the surface of the neutron star, matter can be channeled onto the polar caps. Accreting millisecond X-ray pulsars (AMXP), the subject of this thesis, are a subset of LMXBs in which the spin of the NS is directly observable in this way. The spins of the compact objects in some of the NS LMXBs are also revealed by oscillations observed during thermonuclear bursts [31].

Neutron stars in LMXBs have magnetic fields ($B \sim 10^8 - 10^9$ G) comparable to the magnetic fields of millisecond RPPs and much lower than the magnetic fields of NSs in HMXBs and young RPPs. The physical reason for the magnetic field decay in these objects is not well understood, but it is usually attributed to the very long duration of matter accretion onto these objects.

2.4.2 High-mass x-ray binaries

High-mass X-ray binaries are systems in which the secondary is an early type (O,B, Be) massive star. HMXBs are young systems on the galactic plane where new stars are born. In HMXBs accretion proceeds predominantly through stellar wind driven by the massive companion. If the orbital size of the HMXBs is small enough, a combination of stellar wind and Roche lobe overflow is also possible.HMXBs have a short lifetime ($\sim 10^5 - 10^7$ yr). The NSs in these relatively young systems likely to have strong magnetic fields ($B \sim 10^{12}$ G).

2.5 Neutron Stars in LMXBs

In LMXBs the companion of the accreting NS is usually a late type normal star with a mass range $\sim 0.1 - 1 M_\odot$. Accretion in LMXBs proceeds almost through Roche lobe overflow (see Chapter 3). The lifetimes of LMXBs are determined by the mass-transfer process and therefore are longer ($\sim 10^7 - 10^9$ yr). In comparison neutron stars in LMXBs are thought to have low magnetic fields ($B \sim 10^8 - 10^9$ G) [4].

2.5.1 Accreting millisecond x-ray pulsars

Accreting millisecond X-ray Pulsars (AMXP) are a subset of LMXBs. At the writing of this thesis 13 members have been discovered, the properties of which are shown in the Table 2.1. They are all transient systems in which the system is in quiescence for most of the time due to low mass accretion rate, and becomes detectable during an episode of enhanced accretion. The pulse profiles of AMXPs are sinusoidal. They have low mass companion. The binary orbital period rate ranges between 0.7 and 20 hr for thirteen AMXPs discovered up to date [32].

Table 2.1: The list of accreting millisecond X-ray pulsars. Here, M_c(min) is the minimum mass of companion star.

Star Name	Spin(Hz)	Period(minute)	M_c(min)	Ref
SAX J1808.4-3658	401	120	0.043 $M_\odot$	[3]
SWIFT J1749.4-2807	518	528	0.6 $M_\odot$	[33]
XTE J1807-294	191	40	0.0066 $M_\odot$	[34]
NGC 6440-X2	205	57	0.007 $M_\odot$	[35]
IGR J0029.1+5934	599	150	0.039 $M_\odot$	[36]
XTE J1814-338	314	258	0.17 $M_\odot$	[37]
HETE J1900.1-2455	377	83	0.016 $M_\odot$	[38]
IGR J17511-3057	245	207	0.13 $M_\odot$	[39]
XTE J1751-305	435	42	0.014 $M_\odot$	[40]
SAX J1748.9-2021	442	522	0.1 $M_\odot$	[41]
Aql X-1	550	1140	0.8 $M_\odot$	[42]
SWIFT J1756.9-2508	182	54	0.007 $M_\odot$	[43]
XTE J0929-314	185	44	0.083 $M_\odot$	[44]

Recycling scenario [4] predicts that the NSs observed as millisecond radio pulsars are produced by spin up via the transfer of angular momentum through a very long episode of accretion.

2.5.2 Burst oscillations

Some of the neutron star LMXBs show thermonuclear bursts several times a day suddenly releasing nuclear energy on the timescale of $\sim 10 - 100$ s. This might be the result of thermonuclear instability of the shell of accumulated matter on the NS.

Galloway et al. discovered [45] the presence of oscillations in such bursts and it is understood that [31] the frequency of the oscillations approaches the spin frequency of the NS. These systems are also called nuclear powered millisecond X-ray pulsars. Both SAXJ1808.4−3658 and Aql X−1 show burst oscillations.

2.5.3 Quasi-periodic oscillations

The power density spectrum of AMXPs as well as other LMXBs show broad peaks called quasi-periodic oscillations (QPOs) [46]. These high frequency oscillations most likely arise in the inner disk and allow a diagnostic of the accretion flow in that region [47].

2.5.4 State transitions

Neutron star and black hole systems in LMXBs show spectral changes between hard and soft states. Neutron star spectral state transitions were first observed by Mitsuda et al. [48]. Transition between hard-to-soft state and soft-to-hard state does not occur at the same luminosity. Soft-to-hard state transition luminosity is 5 times lower than hard-to-soft state transition luminosity [8].

The different spectral types can be attributed to different types of accretion flows [49]. The standard Shakura and Sunyaev [50] solution has soft spectrum with high luminosity and can be associated with the high/soft state.

If accretion rate drops below a critical value the inner regions of the disk makes a transition to an optically thin and hot advection dominated accretion flow (ADAF) [51]. Such disks are geometrically thick and their spectra are hard. Such flows then may describe low-hard state [52].

The spectral transitions in black hole and neutron stars systems show very similar behavior and likely originate from the same reason. As black holes do not have magnetospheres, the hysteresis in spectral transitions are not likely to be associated with transition to the propeller stage [5]. This, however, does not contradict the arguments presented in this thesis because neutron stars at low accretion rate are likely to make a transition to the propeller stage accompanying the transition to ADAF.

3. ACCRETION DISKS IN BINARY SYSTEMS

In low mass X-ray binary systems, the matter is predominantly transfered to the disk via Roche lobe overflow rather than stellar wind. In the following section the process of the mass transfer will be described in detail.

3.1 Roche Lobe Overflow

In close binary star systems gravitational forces, the forces due to the orbital motion and rotation of stars have a great importance on the stars shape. We consider two stars with masses M_1 and M_2 rotating in circular orbits about their center of mass in the corotating coordinate system. In a rotating reference frame two stars are at rest, assuming the center of mass is at the origin. The outward push of centrifugal force balances their mutual gravitational attraction.

According to the Kepler's third law, the angular velocity of the binary is given as

$$\omega_{\rm orb} = \left(\frac{GM}{a^3}\right)^{1/2} \tag{3.1}$$

where a is the binary separation and $M = M_1 + M_2$ is the total mass of the system.

Roche potential

$$\Phi_{\rm R}(r) = -\frac{GM_1}{|\mathbf{r}-\mathbf{r_1}|} - \frac{GM_2}{|\mathbf{r}-\mathbf{r_2}|} - \frac{1}{2}(\omega_{\rm orb}\times r)^2 \tag{3.2}$$

where $\mathbf{r}_i$ $(i = 1,2)$ is the position of M_i and $\mathbf{r}$ is the position where the potential is evaluated (see Figure 3.1) includes the potential of each star and a potential term whose gradient gives the pseudo (centrifugal) force that would act on a test particle in the rotating frame. Thus the gradient of the Roche potential gives the forces that would act on a test particle in the rotating frame neglecting the Coriolis forces. The contours (equipotential surfaces) of the Roche potential is shown in Figure 3.2.

The most important, equipotential surface for our discussion, is the **Roche lobe** which is the 8 shaped contour (dumbell shaped in 3 dimensions). If one of the stars fills its

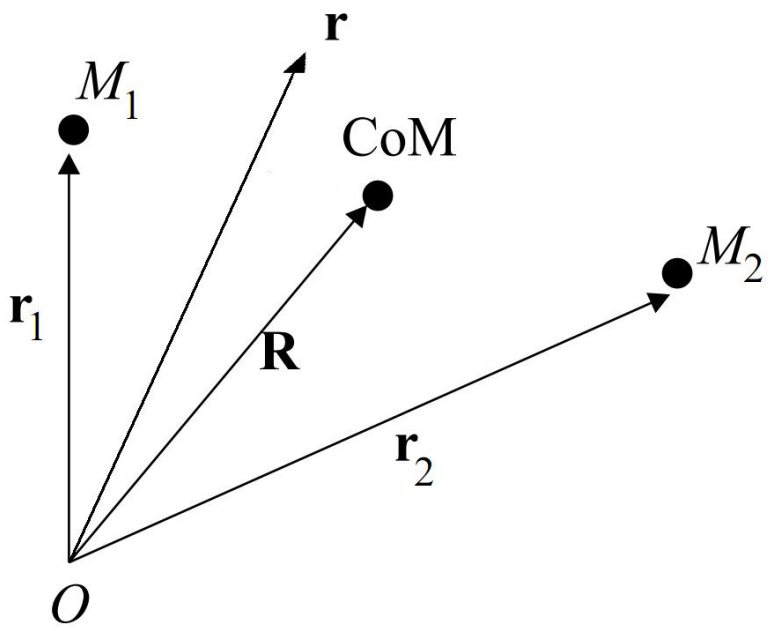

Figure 3.1: Coordinates of the masses in a binary system. The distances r_1 and r_2 are the positions, M_1 and M_2 are the masses of the primary and the secondary of the system, respectively. The centre of mass of the binary system is shown with CoM.

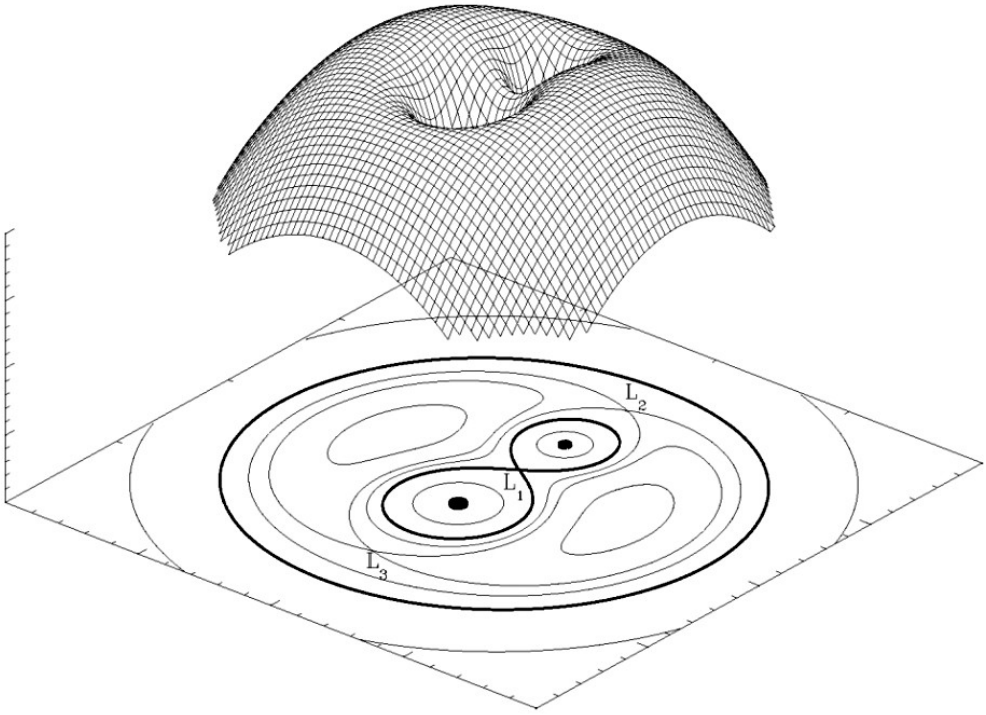

Figure 3.2: Roche lobe geometry in a binary system (from wikipedia).

Roche lobe, the attractive influence of the other star on this excess parts of the star will dominate and matter will be transfered to the companion.

There are five equilibrium points, L_1 to L_5 named after Lagrange. These are all unstable equilibrium points. The most important equilibrium point, for our discussion, is the first Lagrange point, L_1 which is at the intersection point of the 8 shaped Roche lobe.

At some evolutionary stage in a binary system the part of envelope of the secondary star may get close to filling its Roche lobe. If it fills its Roche lobe, the mass transfer will then start from the secondary to the primary through the **Lagrangian point** L_1. This kind of mass transfer is called the **Roche lobe overflow**.

In terms of the orbital period $P_{\rm orb} = 2\pi/\omega_{\rm orb}$ Equation (**3.1**) becomes

$$4\pi^2 a^3 = GMP_{\rm orb}^2 \tag{3.3}$$

For the binary periods of the order of hours a can be expressed as:

$$a = 3.5 \times 10^{10}\,{\rm cm}\, m_1^{1/3}(1+q)^{1/3} P_{\rm hr}^{2/3}, \tag{3.4}$$

where $m_1 = M_1/M_\odot$ and q is the mass ratio defined as

$$q \equiv \frac{M_2}{M_1} \tag{3.5}$$

A useful approximation to the Roche lobe radius which depends on the mass ratio q and binary separation a is

$$\frac{R_2}{a} = \frac{0.49q^{2/3}}{0.6q^{2/3} + \ln(1+q^{1/3})} \tag{3.6}$$

as given by Eggleton [53].

3.2 The Thin Disk

The total mass of the gas in the accretion disk of a LMXB is small compared to the mass of the primary. To a very good approximation the self-gravity of the disk can be neglected. Moreover, the pressure gradients in the radial direction and the radial acceleration term $v\partial v/\partial r$ can be ignored in a thin disk approximation. The circular orbits are then Keplerian, and the angular velocity in the disk is

$$\Omega_{\rm K}(R) = \sqrt{\frac{GM}{R^3}}. \tag{3.7}$$

These conditions cannot be satisfied in the narrow boundary layer region where the angular velocity in the disk matches the angular velocity of the star. As a result the

boundary layer region is not geometrically thin. Such a thin disk can be characterized by vertically averaged quantities like surface mass density Σ i.e. mass per unit surface area of the disk. The equation for the mass conservation is

$$\frac{\partial \Sigma}{\partial t} + \frac{1}{2\pi R}\frac{\partial \dot{M}}{\partial R} = 0 \tag{3.8}$$

where

$$\dot{M} = 2\pi R \Sigma (-V_R) \tag{3.9}$$

is mass inflow rate in the disk and V_R is the radial velocity.

The conservation of angular momentum is

$$\frac{\partial}{\partial t}\left(R^2 \Omega \Sigma\right) + \frac{1}{2\pi R}\frac{\partial \dot{J}}{\partial R} = 0 \tag{3.10}$$

where

$$\dot{J} = R^2 \Omega \dot{M} + 2\pi R^3 \nu \Sigma \frac{\partial \Omega}{\partial R} \tag{3.11}$$

is the angular momentum flux in the disk and ν is the viscosity in the disk.

Using the Keplerian rotation assumption, Equation (**3.7**), the mass conservation and angular momentum equations (**3.8**) and (**3.10**) can be combined in a single equation [54]

$$\frac{\partial \Sigma}{\partial t} = \frac{3}{R}\frac{\partial}{\partial R}\left[R^{1/2}\frac{\partial}{\partial R}\left(R^{1/2}\nu\Sigma\right)\right] \tag{3.12}$$

which is a diffusion equation and is nonlinear if ν depends on Σ.

3.3 Accretion Power

In Newtonian physics the accretion luminosity which approximately corresponds to the X-ray luminosity of the neutron star is

$$L_{\rm X} = \frac{G M_* \dot{M}_*}{R_*} \tag{3.13}$$

where $\dot{M}_*$ is mass accretion rate onto the NS. The observed X-ray flux F_X is related to the X-ray luminosity by

$$F_{\rm X} = \frac{L_{\rm X}}{4\pi d^2}. \tag{3.14}$$

where d is the distance to neutron star.

The luminosity of the disk is

$$L_{\rm disk} = \frac{G M \dot{M}}{2R_{\rm in}} \tag{3.15}$$

if the torque acted on the disk by the star is negligible [55].

3.4 Inner Radius of the Disk

The Alfvén radius is defined as the location where the magnetic pressure

$$P_{\text{mag}} = \frac{B^2}{8\pi} \tag{3.16}$$

is equal to the ram pressure

$$P_{\text{ram}} = \frac{1}{2}\rho v^2. \tag{3.17}$$

For a dipole field, the magnetic field is given by

$$B \simeq \frac{\mu}{r^3} \tag{3.18}$$

where ν is the dipole moment and so the magnetic pressure declines rapidly as

$$P_{\text{mag}} = \frac{\mu^2}{8\pi r^6}. \tag{3.19}$$

For spherical accretion the mass flow rate is

$$\dot{M} = 4\pi r^2 \rho(-v) \tag{3.20}$$

and so

$$|\rho v| = \frac{\dot{M}}{4\pi r^2}. \tag{3.21}$$

The other factor of v in Equation (**3.17**) can be assumed to be equal to the free fall velocity

$$v_{\text{ff}} = \sqrt{\frac{2G\dot{M}_*}{r}} \tag{3.22}$$

and hence the ram pressure can be estimated as

$$P_{\text{ram}} \cong \frac{1}{2}|\rho v| v_{\text{ff}} = \frac{\dot{M}}{8\pi r^2}\sqrt{\frac{2G\dot{M}_*}{r}}. \tag{3.23}$$

By solving

$$P_{\text{ram}}(R_{\text{A}}) = P_{\text{mag}}(R_{\text{A}}) \tag{3.24}$$

one finds

$$R_{\text{A}} = \mu^{4/7}\dot{M}^{-2/7}\left(2GM_*\right)^{-1/7}. \tag{3.25}$$

For disk accretion the inner radius is determined by balancing the magnetic and material stresses. Dimensionally, it depends on μ, $\dot{M}$ and M in a similar way. The

inner radius of the disk is then Alfvén radius up to a dimensionless numerical factor ξ of order unity:

$$R_{\rm in} = \zeta R_{\rm A} \tag{3.26}$$

Ghosh and Lamb finds $\xi \simeq 0.5$ for disk accretion [56]. In terms the typical values for neutron stars, the inner radius of the disk is

$$R_{\rm in} = 1.15 \times 10^9 {\rm cm} \left(\frac{\xi}{0.5}\right) \left(\frac{\dot{M}}{10^{16} {\rm gs}^{-1}}\right)^{-2/7} \mu_{30}^{4/7} \left(\frac{M}{M_\odot}\right)^{-1/7} \tag{3.27}$$

$$= 3.24 \times 10^6 {\rm cm} \left(\frac{\xi}{0.5}\right) \left(\frac{\dot{M}}{10^{16} {\rm gs}^{-1}}\right)^{-2/7} \mu_{26}^{4/7} \left(\frac{M}{M_\odot}\right)^{-1/7}. \tag{3.28}$$

where μ_{30} and μ_{26} are the stellar magnetic moments in units of 10^{30} G cm^3 and 10^{26} G cm^3, respectively. In this thesis I use $\xi = 1$ because I assume that the inner disk region is quasi-spherical [57].

3.5 Corotation Radius

The corotation radius is defined as the radius at which the angular velocity of the star Ω_* is equal to the Keplerian angular velocity in the disk, $\Omega_* = \Omega_{\rm K}(R_{\rm co})$. This can be solved to obtain the corotation radius as

$$R_{\rm co} = \left(\frac{GM_*}{\Omega_*^2}\right)^{1/3} \tag{3.29}$$

In the next chapter this result will be extended to two dimensions by defining the corotation surface.

3.6 Fastness Parameter

The dimensionless fastness parameter is defined as the angular velocity of the star in units of Keplerian angular velocity at the inner radius of the disk

$$\omega_* \equiv \frac{\Omega_*}{\Omega_{\rm K}(R_{\rm in})} \tag{3.30}$$

This can also be written as the ratio of the two characteristic radii

$$\omega_* = \left(\frac{R_{\rm in}}{R_{\rm co}}\right)^{3/2}. \tag{3.31}$$

We define $\dot{M}_{\rm co}$ as the mass flow rate for which the inner radius is equal to the corotation radius, $R_{\rm in} = R_{\rm co}$. This implies

$$\dot{M}_{\rm co} = \frac{\xi^{7/2} \mu^2 \Omega_*^{7/3}}{\sqrt{2} \left(G\dot{M}_*\right)^{5/3}}, \tag{3.32}$$

and the fastness parameter corresponding to mass accretion rate is given by

$$\omega_* = \left(\frac{\dot{M}}{\dot{M}_{\rm co}}\right)^{-3/7}. \tag{3.33}$$

3.7 Accretion Geometry

In spherical coordinates, the geometry of a dipole is given by

$$r = C\sin^2\theta \tag{3.34}$$

where C is a constant labeling different field lines. Considering the point where $r = R_{\rm in}$ for $\theta = 90^\circ$ it is found that $C = R_{\rm in}$. So the dipole field connecting the inner radius of the disk to the star is

$$r = R_{\rm in}\sin^2\theta \tag{3.35}$$

This field line crosses the stellar surface at $r = R_*$ at colatitude $\theta_{\rm c}$ given by

$$\sin^2\theta_{\rm c} = \frac{R_*}{R_{\rm in}} \tag{3.36}$$

The area of a polar cap is $2\pi R_*^2(1-\cos\theta_{\rm c})$. As there are two polar caps, the area of accreting region is

$$A_{\rm c} = 4\pi R_*^2\left(1-\sqrt{1-\frac{R_*}{R_{\rm in}}}\right) \tag{3.37}$$

If $R_* \ll R_{\rm in}$, this simplifies as $A_{\rm c} = 2\pi R_*^3/R_{\rm in}$. For AMXPs this simplification can not be justified as they have relatively weak dipole fields and thus small inner disk radii.

3.8 Accretion Torques and Spin Evolution

The first estimates of the accretion torque [58–60] on the star give an explanation on how centrifugal barrier prevents accretion if star rotates faster than the innermost disk matter. The matter in the disk rotates in almost Keplerian orbits with angular velocity given in Equation (**3.7**).

The specific angular momentum is, i.e., the angular momentum per unit mass of the disk matter is given by,

$$l = R^2\Omega_{\rm K}(R) = \sqrt{GMR}. \tag{3.38}$$

The specific angular momentum of matter carried at $R_{\rm in}$ is

$$l_{\rm in} = \sqrt{GMR_{\rm in}} \tag{3.39}$$

Thus the accreting matter exerts an torque on the star, assuming that $\dot{M} = \dot{M}_*$

$$N_0 = \dot{M}\sqrt{GMR_{\rm in}}. \tag{3.40}$$

where $\dot{M}$ is the mass flow rate and $\dot{M}_*$ is the mass accretion rate. The stellar angular momentum is

$$J_* = I_*\Omega_* \tag{3.41}$$

The value of any accretion torque corresponding to specific angular momentum is

$$N \equiv \dot{M}l \tag{3.42}$$

Differentiating J_* with respect to time

$$\frac{\dot{\Omega}_*}{\Omega_*} = \frac{\dot{M}}{M_*}\left(\frac{l}{l_*} - \frac{d\ln I_*}{d\ln M_*}\right) \tag{3.43}$$

where

$$l_* \equiv \frac{J_*}{M_*}. \tag{3.44}$$

Assuming that the rotational angular momentum of NS is in the same direction as orbital angular momentum then all angular momentum have the same sign in Equation (**3.43**). If l/l_* exceeds logarithmic derivative, the star spins up because of accretion and it is seen that $\dot{\Omega} > 0$. If the logarithmic derivative in Equation (**3.43**) is dominant, then the star spins down.

As a result of small magnetic fields the accretion torques on AMXP are small. In this thesis we do not consider the change in the pulse frequency of AMXPs by accretion torques or by any other means. During an outburst the change in the fastness parameter due to change in the spin period is negligible compared to the changes in the same parameter due to changes in the mass flow rate.

4. ACCRETION IN THE SPIN-DOWN REGIME

Following an outburst the mass flow rate in the disk declines three orders of magnitude. As the mass flow rate declines, the inner radius of the disk

$$R_{\rm in} = \left(\frac{\mu^2 \sqrt{GM}}{\sqrt{2} L_{\rm X} R} \right)^{2/7} \tag{4.1}$$

where $L_{\rm X} = GM\dot{M}/R$ might go beyond the corotation radius

$$R_{\rm co} = \left(\frac{GM}{4\pi^2} \right)^{1/3} P^{2/3} \tag{4.2}$$

where P is the rotational period of the NS. At this stage, $\omega_* > 1$, the Keplerian angular velocity at the inner disk is smaller than the angular velocity of the magnetosphere and the angular momentum is transfered from the star to the disk [58]. The transition will take place at the critical luminosity [60]

$$L_{\rm c} = \frac{\left(4\pi^2\right)^{7/6} \mu^2}{\sqrt{2} R \left(GM\right)^{2/3} P^{7/3}} \tag{4.3}$$

obtained by equating the inner and corotation radii given above. In the spin-down regime, because of the centrifugal barrier, the material can not accrete onto the neutron star and is propelled by its magnetosphere. As a result the accretion onto the magnetic poles is expected to cease, the X-ray luminosity is expected to drop abruptly and the X-ray pulsations then are not expected to be observed. This "propeller effect" [5,61,62] has been considered since 1970s.

Specifically, the intermittent pulsar Aql X-1 has been suggested to be the best candidate for displaying the properties of propellers [63, 64]. In the conventional propeller models there exists a single critical luminosity, given in Equation (**4.3**), at which transition to the propeller stage and back to the accretion stage occurs. Maccarone in 2003 observed an hysteresis effect in which the transition to the high luminosity regime takes place at a luminosity that is different from the luminosity at which the transition to the low luminosity regime occurs [8]. This, according to [8] challenges transition to the propeller stage as an explanation of the rapid drop in luminosity.

The X-ray luminosity of an AMXP, during an outburst, changes two orders of magnitude. These objects can accrete matter even for very low accretion rates for which the inner radius would be beyond the corotation radius [65]. Pulsations persist as long as the intensity is above the detection limit. The object keeps accreting in the spindown regime [66]. Apparently, the propeller regime does not set in abruptly at a critical value of the accretion rate. In order to adress this problem [65] argued that the disk structure around the magnetosphere will adjust itself so that the inner radius of the disk will remain fixed near the corotation radius allowing accretion to continue.

Indeed, if the inner region of the disk is infinitely thin then no accretion is possible should the inner radius go beyond the corotation radius. If, on the other hand, the inner disk is thick, it is then possible that some fraction of matter above the disk plane can accrete onto the star while the matter on the disk plane is propelled. In this thesis we explore this alternative explanation. This has the advantage that it does not require the inner disk to remain fixed while the mass flow rate declines during the outburst. Furthermore, partial accretion can adddress the rapid decline stage that we will explain later. In the following original part of the thesis, we investigate this partial accretion regime and apply the model on AMXPs.

4.1 Partial Accretion in the Propeller Regime

Accretion in the spin down regime received much less attention than, for example, the torques that should act. Lipunov studied the fraction of mass that can accrete onto a rapidly rotating star under spherical accretion [6]. Menou et al. considered the quasi-spherical accretion case in the propeller regime [7] employing an advection dominated accretion flow ADAF model [51,57]. More recently, [67,68] have studied accretion in the spin down regime. In Çeşme, ASTRONS meeting we presented the consequences of this model on the outburst lightcurve of SAX J1808.4−3658 [1].

4.1.1 Corotation surface

In Chapter 3 we defined the corotation radius at the disk plane. It is possible to generalize this concept to two dimensions. Consider a test particle at spherical coordinates (r,θ) rotating with the magnetosphere. The distance of this particle to the rotation axis is then

$$r_\perp = r\sin\theta \tag{4.4}$$

and the centrifugal acceleration is

$$a_\mathrm{c} = -\Omega_*^2 r\sin\theta. \tag{4.5}$$

The acceleration at the radial direction is

$$a_\mathrm{r} = a_\mathrm{c}\sin\theta = -\Omega_*^2 r\sin^2\theta \tag{4.6}$$

The corotation surface r_c is defined as the locus of points where the gravitational acceleration $g_\mathrm{r} = -GM_*/r^2$ is equal to the radial acceleration:

$$\Omega_*^2 r_\mathrm{c}\sin^2\theta = \frac{GM_*}{r_\mathrm{c}^2}. \tag{4.7}$$

This can be arranged to give the corotation surface

$$r_\mathrm{c} = R_\mathrm{c}\sin^{-2/3}\theta \tag{4.8}$$

where R_c is the usual corotation radius on the disk plane.

4.1.2 Partial accretion

The intersection of the corotation surface with the Alfvén surface (defined soon) defines a critical angle θ_0. Matter inside the cone with $\theta < \theta_0$ is not centrifugally inhibited and can accrete onto the NS. This fraction can be calculated through

$$f \equiv \frac{\dot{M}_*}{\dot{M}} = \frac{2\int_0^{\theta_0} 2\pi r^2\sin\theta\rho v d\theta}{2\int_0^{\pi/2} 2\pi r^2\sin\theta\rho v d\theta}. \tag{4.9}$$

where $\rho = \rho(r,\theta)$ and $v = v(r,\theta)$ in general [7]. Note that this boils down to evaluating

$$f \equiv \frac{\int_0^{\theta_0}\sin\theta\rho v d\theta}{\int_0^{\pi/2}\sin\theta\rho v d\theta} \tag{4.10}$$

in the general case.

4.1.3 Alfvén surface in the spherical accretion case

In Chapter 3 we have defined the Alfvén radius as

$$R_{\rm A} = \left(\frac{\mu^2}{\sqrt{2GM}\dot{M}} \right)^{2/7}. \tag{4.11}$$

It is possible generalize this concept to two dimensions. This we do here for aligned rotators accreting spherically. In this case the poloidal components of the magnetic fields are

$$B_{\rm r} = \frac{2\mu}{r^3}\cos\theta \tag{4.12}$$

$$B_{\theta} = \frac{\mu}{r^3}\sin\theta. \tag{4.13}$$

Accordingly, the magnetic pressure, $B^2/8\pi$, is

$$P_{\rm mag} = \frac{\mu^2}{8\pi r^6}\left(1+3\cos^2\theta\right). \tag{4.14}$$

Recalling that the ram pressure is

$$P_{\rm ram} = \frac{\dot{M}}{8\pi r^2}\sqrt{\frac{2GM_*}{r}} \tag{4.15}$$

we obtain the Alfvén surface as

$$r_{\rm A} = R_{\rm A}\left(1+3\cos^2\theta\right)^{2/7}. \tag{4.16}$$

Note that this reduces to the usual result $r_{\rm A} = R_{\rm A}$ at the disk plane ($\theta = \pi/2$).

4.1.4 Fraction of mass accreting in the spherical accretion case

Partial accretion in the propeller stage, for spherical accretion was first studied by Lipunov [6]. The equilibrium of the Alfvén surface, given in Equation (**4.16**), with the corotation surface, given in Equation (**4.8**), defines the critical angle θ_0

$$\left(1+3\cos^2\theta_0\right)^{3/7}\sin\theta_0 = \omega_*^{-1} \tag{4.17}$$

at a certain fastness parameter. As ρ and v does not depend on θ (spherical accretion) Equation (**4.10**) evaluates to

$$f = \frac{\int_0^{\theta_0}\sin\theta d\theta}{\int_0^{\pi/2}\sin\theta d\theta} = 1-\cos\theta_0. \tag{4.18}$$

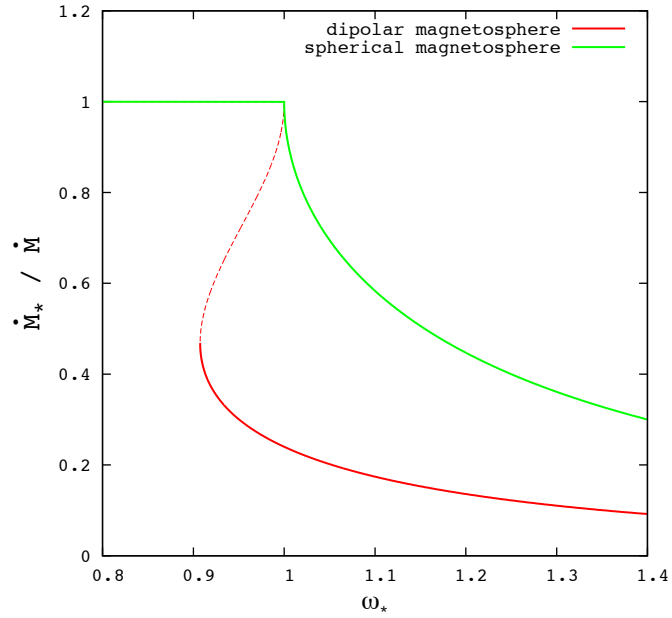

Figure 4.1: Fraction of mass flow rate that accrete for spherical case. The green curve represents the fraction obtained for spherical magnetosphere given in Equation (**4.21**). The red curve, parametrically defined in Equation (**4.19**), is for dipolar shaped magnetosphere. The dashed segment is the region for which $df/d\omega_* > 0$ and will not be realized. This presents a theoretical framework in which the transitions between accretion and propeller stages can occur at different luminosities, as we discuss in the next section.

This, together with Equation (**4.17**) determines the fraction f that can accrete as a function of the fastness parameter. Thus $f = f(\omega_*)$ is defined parametrically through the parameter $s = \cos\theta_0$ as

$$\omega_* = \frac{1}{(1+3s^2)^{3/7}\sqrt{1-s^2}}, \qquad f = 1-s \tag{4.19}$$

If one assumes that the magnetosphere is spherical, i.e. $r_A \simeq R_A$, then Equation (**4.17**) simplifies as

$$\sin\theta_0 = \omega_*^{-1} \tag{4.20}$$

and the fraction of accreting matter can be written explicitly as

$$f = 1 - \sqrt{1-\omega_*^{-2}} \tag{4.21}$$

This, together with the exact solution given in Equation (**4.19**) is shown in Figure 4.1.

It is seen that the exact solution is doubly-valued for the range of fastness parameters $\omega_{c1} < \omega_* < 1$ where $\omega_{c1} = 0.90748$ obtained for $\cos\theta_0 = \sqrt{11/39}$. The region $df/d\omega_* > 0$ (shown with dashed lines) will not be realized because on general grounds

one expects that the fraction that can accrete should decrease with increasing fastness parameter. As I discuss in the next section, f being doubly valued presents a theoretical framework in which the transitions between accretion and propeller stages can occur at different luminosities.

4.1.5 Quasi-spherical accretion case

Here I follow the work of Menou et al. [7] who derived the fraction of accreting matter in the quasi-spherical case. Relying on [57] they assume

$$v = v_r(r,\theta) \simeq v_r(r)\sin^2\theta \tag{4.22}$$

$$\rho = \rho(r,\theta) \simeq \rho(r) \tag{4.23}$$

and the fraction that can accrete is

$$\begin{aligned} f &= \frac{\dot{M}_*}{\dot{M}} = \frac{2\int_0^{\theta_0} 2\pi r^2 \sin\theta \rho(r) v_r(r) \sin^2\theta d\theta}{2\int_0^{\pi/2} 2\pi r^2 \sin\theta \rho(r) v_r(r) \sin^2\theta d\theta} = \frac{\int_0^{\theta_0} \sin^3\theta d\theta}{\int_0^{\pi/2} \sin^3\theta d\theta} \\ &= 1 - \frac{3}{2}\cos\theta_0 + \frac{1}{2}\cos^3\theta_0 \end{aligned} \tag{4.24}$$

where we assumed that matter inside the corotation surface $\theta < \theta_0$ can accrete.

In the disk accretion case the inner radius of the disk is determined by balancing the magnetic and material stresses rather than magnetic and ram pressures. The material stress $\rho v_r v_\phi$ has a factor of $\sin^2\theta$ because of the v_r term. Given the uncertainty in the vertical structure of the disk and the fact that we already have ignored the screening currents that would be produced in the disk, we simply follow the approach employed in spherical accretion case

$$r_{\rm A} = R_{\rm A}\left(1 + 3\cos^2\theta\right)^{2/7}. \tag{4.25}$$

Equilibrium of this with the corotation surface given in Equation (**4.8**) parametrically defines $f(\omega_*)$ through

$$\omega_* = \frac{1}{(1+3s^2)^{3/7}\sqrt{1-s^2}}, \qquad f = 1 - \frac{3}{2}s + \frac{1}{2}s^3. \tag{4.26}$$

where $s \equiv \cos\theta$ as before.

Using the spherical magnetosphere approximation $\sin\theta_0 = \omega_*^{-1}$ the fraction that can accrete is

$$f = 1 - \frac{3}{2}\left(1-\omega_*^{-2}\right)^{1/2} + \frac{1}{2}\left(1-\omega_*^{-2}\right)^{3/2} \tag{4.27}$$

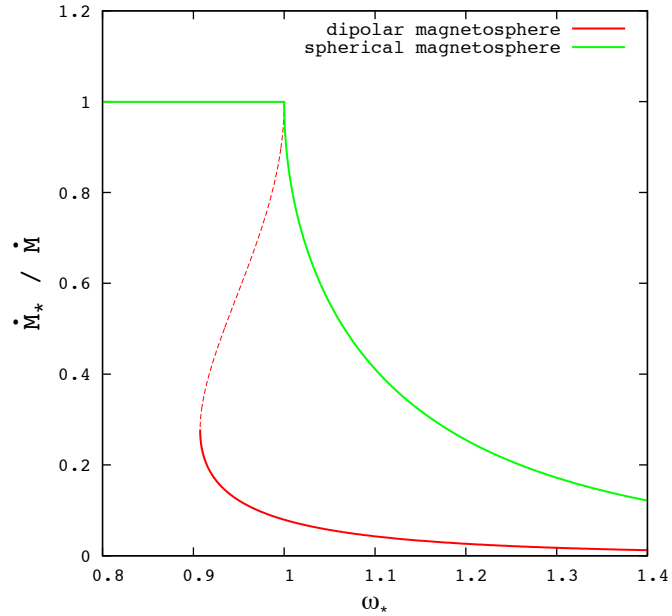

Figure 4.2: Fraction of mass flow rate that accrete for quasi-spherical case. The green curve represents the fraction obtained for spherical magnetosphere given in Equation (**4.27**). The red curve, parametrically defined in Equation (**4.26**), is for dipole shaped magnetosphere. The dashed segment is the region for which $df/d\omega_* > 0$ and will not be realized.

This together with the exact solution given in Equation (**4.26**) is shown in Figure 4.2. Again, one sees that employing the dipolar shape of the magnetosphere rather than assuming it to be spherical, we obtain doubly valued $f(\omega_*)$. This, as I argue in the next section allows for a hysteresis behavior. In the next section we generalize this calculation for non-aligned rotators.

4.2 Magnetic Radius and Partial Accretion For Non-aligned Rotators

In this section we consider accretion during spin down regime for non-aligned rotators. If there is an inclination angle α between the rotation and magnetic axis, the components of the magnetic dipole field can be written in spherical coordinates as

$$\begin{aligned} B_{\rm r} &= \frac{2\mu}{r^3}(\cos\alpha\cos\theta + \sin\alpha\sin\theta\cos(\phi - \Omega_* t)) \\ B_\theta &= \frac{\mu}{r^3}(\cos\alpha\sin\theta - \sin\alpha\cos\theta\cos(\phi - \Omega_* t)) \\ B_\phi &= \frac{\mu}{r^3}\sin\alpha\sin(\phi - \Omega_* t) \end{aligned} \qquad \textbf{(4.28)}$$

as given in [69].

If the square of the field components are averaged over a period, the ϕ dependence disappears and I obtain

$$\left\langle B_{\rm r}^2 \right\rangle = \left(\frac{2\mu}{r^3}\right)^2 \left(\cos^2\alpha\cos^2\theta + \frac{1}{2}\sin^2\alpha\sin^2\theta\right) \quad \textbf{(4.29)}$$

$$\left\langle B_{\theta}^2 \right\rangle = \left(\frac{\mu}{r^3}\right)^2 \left(\cos^2\alpha\sin^2\theta + \frac{1}{2}\sin^2\alpha\cos^2\theta\right) \quad \textbf{(4.30)}$$

$$\left\langle B_{\phi}^2 \right\rangle = \left(\frac{\mu}{r^3}\right)^2 \frac{1}{2}\sin^2\alpha \quad \textbf{(4.31)}$$

The average value of the square of the field is then the sum of these components

$$\left\langle B^2 \right\rangle = \left(\frac{\mu}{r^3}\right)^2 \left[\left(3\cos^2\theta - 1\right)\frac{3}{2}\cos^2\alpha + \frac{5}{2} - \frac{3}{2}\cos^2\theta\right] \quad \textbf{(4.32)}$$

Balancing the magnetic pressure with the ram pressure gives

$$r_{\rm A} = R_{\rm A}\left[\left(3\cos^2\theta - 1\right)\frac{3}{2}\cos^2\alpha + \frac{5}{2} - \frac{3}{2}\cos^2\theta\right]^{2/7}. \quad \textbf{(4.33)}$$

Equating this with the corotation surface $r_{\rm c} = R_{\rm c}\sin^{-2/3}\theta$ given in Equation (**4.8**) results

$$\left[\left(3\cos^2\theta - 1\right)\frac{3}{2}\cos^2\alpha + \frac{5}{2} - \frac{3}{2}\cos^2\theta\right]^{3/7}\sin\theta = \frac{1}{\omega_*} \quad \textbf{(4.34)}$$

This parametrically defines $f(\omega_*)$ through

$$\omega_* = \left[\left(3s^2 - 1\right)\frac{3}{2}\cos^2\alpha + \frac{5}{2} - \frac{3}{2}s^2\right]^{-3/7}\left(1 - s^2\right)^{-1/2}, \qquad f = 1 - \frac{3}{2}s + \frac{1}{2}s^3. \quad \textbf{(4.35)}$$

Using the spherical magnetosphere approximation $\sin\theta_0 = \omega_*^{-1}$ the fraction that can accrete is

$$f = 1 - \frac{3}{2}\left(1 - \omega_*^{-2}\right)^{1/2} + \frac{1}{2}\left(1 - \omega_*^{-2}\right)^{3/2} \quad \textbf{(4.36)}$$

This together with the exact solution given in Equation (**4.35**) is shown in Figure 4.3

It is generally assumed that transition from accretion to the propeller stage starts at a critical fastness parameter $\omega_c = 1$. In this model, however, partial accretion ($f < 1$) begins when $\theta_0 = \pi/2$ in Equation (**4.33**). This gives critical fastness parameter as

$$\omega_{\rm c} = \left(\frac{5}{2} - \frac{3}{2}\cos^2\alpha\right)^{-3/7} \quad \textbf{(4.37)}$$

For $\alpha = \pi/2$ the critical fastness parameter is found as $\omega_{\rm c} = 0.67523$.

We see that the curves for all inclination angles pass from a certain single point. The reason is as follows: The Equation (**4.33**) does not have dependence on inclination

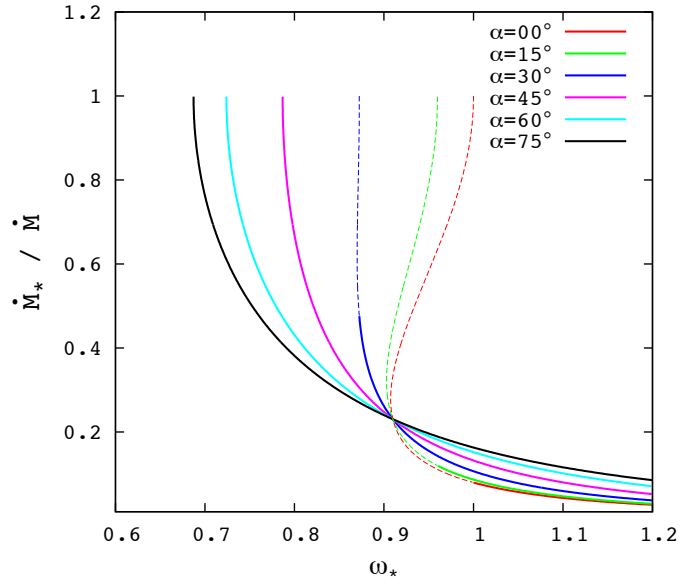

Figure 4.3: Fraction of mass flow rate that can accrete for a range of inclination angle α between rotation and magnetic axis.It is seen that f is doubly valued for small inclination angles.

angle α for the value of $\cos^2\theta_0 = \frac{1}{3}$. This happens when the fastness parameter is equal $\omega_* = 0.91$.

The regions where $d\omega_*/df$ have different sign depend on the inclination angle as

$$\cos^2\theta_0 = \frac{1}{39}\frac{75\cos^2\alpha - 53}{3\cos^2\alpha - 1} \tag{4.38}$$

This gives a critical angle $\alpha_c = 32^\circ$ defined through $\cos\alpha_c = \sqrt{53/75}$, below which f is multiply defined.

When the inclination angle is small and f is doubly valued it is possible to obtain hysteresis behavior in transitions between accretion and propeller stages. During the slow decay stage of an outburst $f = 1$. As the mass flow rate decreases the fastness parameter increases. At some stage it will exceed ω_c and partial accretion will commence. However, beyond point A in Figure 4.4 $df/d\omega_* > 0$ on the curve and f will drop abruptly to point B along the arrow and drop further if the fastness parameter increases. When the accretion rate is increasing (such as at the rising phase of an outburst) f will increase until point C and jump to point D where $f = 1$. As the points A and C where transitions to the propeller and accretion regimes take place correspond to different f values, the luminosities at these points are different.

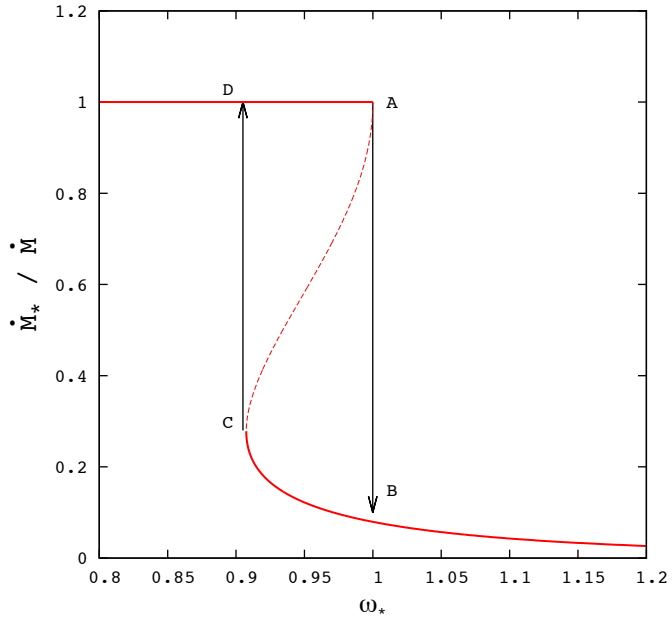

Figure 4.4: A schematic description of how the hysteresis behavior in transitions can be addressed. The system follows the path A-B-C-D and accordingly the transition from the accretion to the propeller regime does not take place at the luminosity at which transition from the propeller to the accretion regime occurs.

4.3 The Origin of the Hysteresis Behavior

In previous section we have seen that $f(\omega_*)$ can be doubly valued for small inclination angles so that transitions from accretion to propeller regime and back (from propeller to accretion regime) occur at different luminosities. The question naturally arises what makes low inclination angles different than higher ones. The answer should be related to the shape of the magnetosphere as the shape of the corotation surface does not change with the inclination angle. The period averaged shape of the magnetosphere changes with the inclination angle, elongated for the small inclination angles becomming flatter as the inclination angles becomes larger. The double-valuedness of f and the resulting hysteresis behavior must be addressed through this elongated shape for small inclination angles.

The Equation (**4.33**) implies that the radius of magnetosphere $R_{\rm m}$ at the disk plane $(\theta = \pi/2)$ is

$$R_{\rm m} = R_{\rm A}\left(\frac{5}{2} - \frac{3}{2}\cos^2\alpha\right)^{2/7}. \qquad (\mathbf{4.39})$$

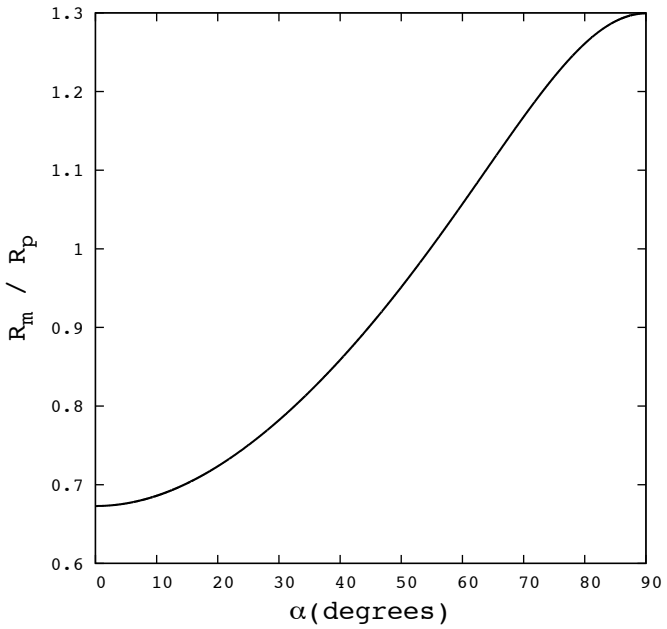

Figure 4.5: The ratio of $R_{\rm m}/R_{\rm p}$, a measure of the flatness of the magnetosphere, as a function of the inclination angle α. The magnetosphere is elongated only for small inclination angles.

Similarly, the radius of the magnetosphere at the rotation axis ($\theta = 0^\circ$) is

$$R_{\rm p} = R_{\rm A}\left(3\cos^2\alpha + 1\right)^{2/7}. \qquad \textbf{(4.40)}$$

The ratio of $R_{\rm m}/R_{\rm p}$ is

$$\frac{R_{\rm m}}{R_{\rm p}} = \left(\frac{1}{2}\frac{5-3\cos^2\alpha}{1+3\cos^2\alpha}\right)^{2/7} \qquad \textbf{(4.41)}$$

and is shown in Figure 4.5. As $R_{\rm m}/R_{\rm p}$ measure the flatness of the magnetosphere, the Figure makes it evident that flatness increases with the inclination angle.

5. APPLICATION TO SAX J1808.4-3658

According to the model presented in this thesis there are two types of lightcurves. For large inclination angles (larger than 32°) transition to the rapid decay stage occurs continuously as the fastness parameter increases. There is no hysteresis behavior when the fastness parameter changes and the system makes a transition to the accretion stage again.

Such a continuous transition to the rapid decay stage can address, for example, the lightcurve of the accreting millisecond X-ray pulsar SAX J1808.4−3658. The X-ray light curve of SAX J1808.4−3658 has four stages shown in Figure 5.1 as taken from [1]. We are interested in peak, slow decay and rapid decay stages. Peak luminosity is $F_x \approxeq 2.7 \times 10^{-9} erg$ cm$^{-2} s^{-1}$ for 3-20 keV energy band. We have modeled the first three stages of this lightcurve by the model described in the previous section. In the rapid decay stage we assume a fraction f, parametrically defined in Equation (**4.34**), accretes onto the star. The luminosity is then

$$L = \frac{GM\dot{M}_{\text{in}} f}{R_*} \tag{**5.1**}$$

The result is is given in Figure 5.2.

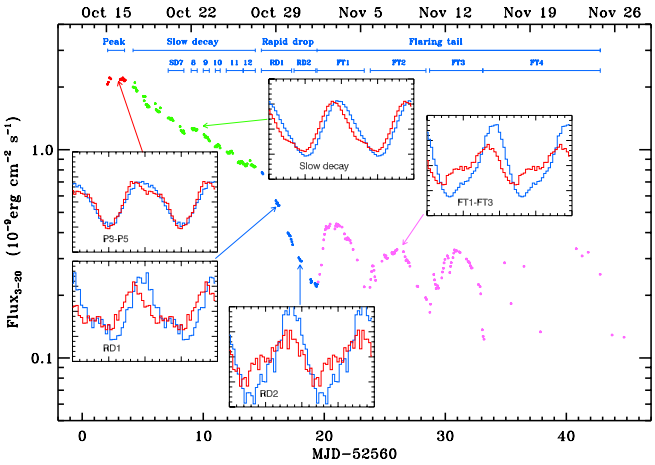

Figure 5.1: 2002 outburst lightcurve of SAX J1808.4−3658. From Ibragimov and Poutanen 2009.

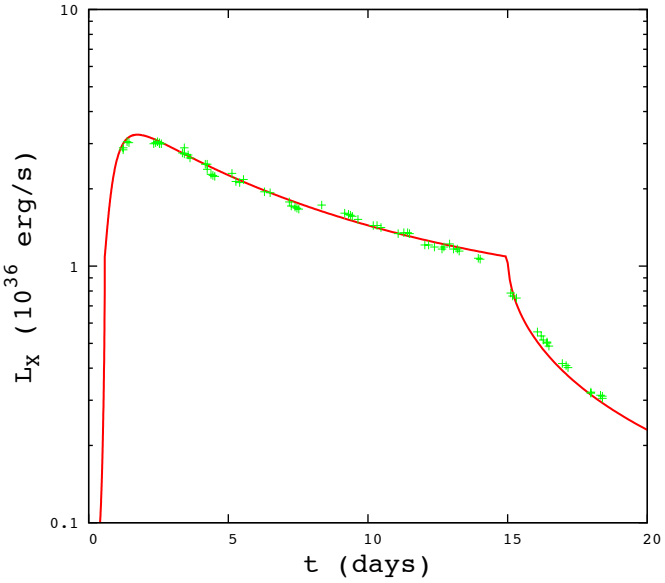

Figure 5.2: Modelling the 2002 outburst lightcurve of SAX J1808.4−3658. The data taken from [1] given here in Figure 5.1. We assumed an inclination angle of 36° and magnetic moment $\mu = 0.618 \times 10^{26}$ G cm^3.

The second type of lightcurve, is obtained for small inclination angles, (smaller than 32°) in the model presented in this thesis. In these cases the luminosity should decline discontinuously when the system makes a transition to the propeller stage. As in this case f is doubly valued it is possible to obtain hysteresis behavior. Transition back to the accretion stage will not occur at the same luminosity. Instead, f will increase along the curve as long as $df/d\omega_* < 0$. It will jump back to the full accretion stage at the point where $d\omega_*/df = 0$.

This type of model can explain the lightcurve of Aql X-1. The lightcurve of 1997 outburst of Aql X-1 [70] has rapid drop during transition to the propeller stage as shown in Figure 5.3. The luminosity at this stage is $\sim 10^{33}$ erg s^{-1}. The fit on the figure is by the authors of the original paper.

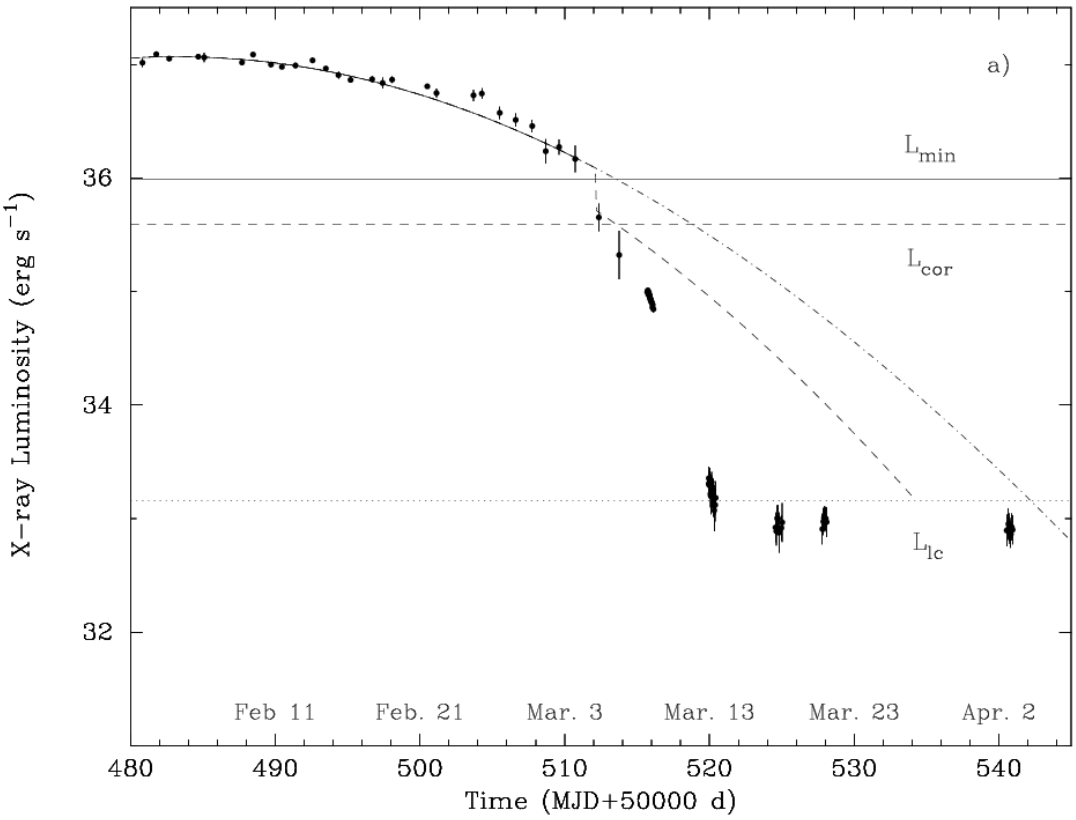

Figure 5.3: 1997 outburst lightcurve of Aql X-1. From Campana and Stella 2003 [2].

6. CONCLUSIONS

In this thesis the fraction of the mass flow rate that can reach the surface of the neutron star in the propeller stage is calculated depending on the fastness parameter and the inclination angle between magnetic and rotation axis. This result is shown in Figure 4.3. According to this result, the fraction that can accrete decreases with increasing fastness parameter, and increases with the inclination angle, as expected.

Originally, a critical fastness parameter, beyond which the partial accretion ($f < 1$) is possible, presented in Equation (**4.37**), is shown to decrease with the inclination angle is. For aligned rotators ($\alpha = 0$) the critical fastness parameter is 0.99 and for rotators with an inclination angle of $\alpha_c = 32^\circ$ the critical fastness is 0.67.

For small inclination angles ($\alpha < \alpha_c$) it is found that the critical fastness parameter for transition from full accretion to partial accretion regime can be different from the critical fastness parameter for transition from the partial accretion regime to the full accretion regime. This hysteresis effect can be associated with the observations of some of the systems (Aql X-1) during outburst.

In this thesis accretion in the propeller stage is associated with the rapid decay stage of accreting millisecond pulsars. This idea is used to model the outburst lightcurve of SAX J1808.4-3658.

There are critical assumptions in the model that can effect the results. We have employed a very specific disk model [57] for the vertical structure (the θ dependence) of the disk. This assumption should be relaxed and other models might be checked to see whether our results are robust.

A very simplifying assumption was to employ the dipole geometry for the magnetosphere of the neutron star which is to be modified by the presence of the disk. We intend to consider self-consistent magnetospheric structure in the presence of the disk in the future.

Although the critical inclination angle that we have found ($\alpha_c = 32^\circ$) will probably be altered with the improvement of the model along the lines mentioned above, we firmly believe that any elongated shape of the magnetosphere will ensure the hysteresis effect described in this thesis.

REFERENCES

[1] **Ibragimov, A. and Poutanen, J.**, 2009. Accreting millisecond pulsar SAX J1808.4-3658 during its 2002 outburst: evidence for a receding disc, *Monthly Notices of Royal Astronomical Society*, **400**, 492–508, *0901.0073*.

[2] **Campana, S. and Stella, L.**, 2003. The Evolution of the High-Energy Tail in the Quiescent Spectrum of the Soft X-Ray Transient Aquila X-1, *Astrophysical Journal*, **597**, 474–478, *arXiv:astro-ph/0307218*.

[3] **Wijnands, R. and van der Klis, M.**, 1998. A millisecond pulsar in an X-ray binary system, *Nature*, **394**, 344–346.

[4] **Alpar, M.A.**, **Cheng, A.F.**, **Ruderman, M.A. and Shaham, J.**, 1982. A new class of radio pulsars, *Nature*, **300**, 728–730.

[5] **Illarionov, A.F. and Sunyaev, R.A.**, 1975. Why the Number of Galactic X-ray Stars Is so Small?, *Astronomy and Astrophysics*, **39**, 185.

[6] **Lipunov, V.M. and Shakura, N.I.**, 1976. On the nature of binary-system X-ray pulsars, *Soviet Astronomy Letters*, **2**, 133–135.

[7] **Menou, K.**, **Esin, A.A.**, **Narayan, R.**, **Garcia, M.R.**, **Lasota, J. and McClintock, J.E.**, 1999. Black Hole and Neutron Star Transients in Quiescence, *Astrophysics Journal*, **520**, 276–291, *arXiv:astro-ph/9810323*.

[8] **Maccarone, T.J. and Coppi, P.S.**, 2003. Hysteresis in the light curves of soft X-ray transients, *Monthly Notices of Royal Astronomical Society*, **338**, 189–196, *arXiv:astro-ph/0209116*.

[9] **Tolman, R.C.**, 1939. Static Solutions of Einstein's Field Equations for Spheres of Fluid, *Physical Review*, **55**, 364–373.

[10] **Oppenheimer, J.R. and Volkoff, G.M.**, 1939. On Massive Neutron Cores, *Physical Review*, **55**, 374–381.

[11] **Lyne, A.G. and Graham-Smith, F.**, 2006. Pulsar Astronomy, Cambridge.

[12] **Frank, J.**, **King, A. and Raine, D.**, 2002. Accretion Power in Astrophysics, Cambridge University Press, 3 edition, *http://amazon.com/o/ASIN/0521629578/*.

[13] **Taylor, Jr., J.H.**, 1991. Millisecond pulsars - Nature's most stable clocks, *IEEE Proceedings*, **79**, 1054–1062.

[14] **Mereghetti, S.**, 2008. The strongest cosmic magnets: soft gamma-ray repeaters and anomalous X-ray pulsars, *Annual Reviews of Astronomy and Astrophysics*, **15**, 225–287, *0804.0250*.

[15] **Backer, D.C.**, **Kulkarni, S.R.**, **Heiles, C.**, **Davis, M.M. and Goss, W.M.**, 1982. A millisecond pulsar, *Nature*, **300**, 615–618.

[16] **Baade, W. and Zwicky, F.**, 1934. On Super-novae, *Proceedings of the National Academy of Science*, **20**, 254–259.

[17] **Hewish, A.**, **Bell, S.J.**, **Pilkington, J.D.H.**, **Scott, P.F. and Collins, R.A.**, 1968. Observation of a Rapidly Pulsating Radio Source, *Nature*, **217**, 709–713.

[18] **Giacconi, R.**, **Gursky, H.**, **Kellogg, E.**, **Schreier, E. and Tananbaum, H.**, 1971. Discovery of Periodic X-Ray Pulsations in Centaurus X-3 from UHURU, *Astrophysical Journal Letters*, **167**, L67.

[19] **Radhakrishnan, V. and Srinivasan, G.**, 1982. On the origin of the recently discovered ultra-rapid pulsar, *Current Science*, **51**, 1096–1099.

[20] **Pacini, F.**, 1967. Energy Emission from a Neutron Star, *Nature*, **216**, 567–568.

[21] **Gold, T.**, 1968. Rotating Neutron Stars as the Origin of the Pulsating Radio Sources, *Nature*, **218**, 731–732.

[22] **Gold, T.**, 1969. Rotating Neutron Stars and the Nature of Pulsars, *Nature*, **221**, 25–27.

[23] **Alpar, M.A.**, 2001. On Young Neutron Stars as Propellers and Accretors with Conventional Magnetic Fields, *Astrophysical Journal*, **554**, 1245–1254, *arXiv:astro-ph/0005211*.

[24] **Chatterjee, P.**, **Hernquist, L. and Narayan, R.**, 2000. An Accretion Model for Anomalous X-Ray Pulsars, *Astrophysical Journal*, **534**, 373–379, *arXiv:astro-ph/9912137*.

[25] **Ekşi, K.Y. and Alpar, M.A.**, 2003. Can Thin Disks Produce Anomalous X-Ray Pulsars?, *Astrophysical Journal*, **599**, 450–456, *arXiv:astro-ph/0308455*.

[26] **Ertan, Ü. and Alpar, M.A.**, 2003. On the Enhanced X-Ray Emission from SGR 1900+14 after the August 27 Giant Flare, *Astrophysical Journal Letters*, **593**, L93–L96, *arXiv:astro-ph/0307344*.

[27] **Wang, Z.**, **Chakrabarty, D. and Kaplan, D.L.**, 2006. A debris disk around an isolated young neutron star, *Nature*, **440**, 772–775, *arXiv:astro-ph/0604076*.

[28] **Rea, N.**, **Esposito, P.**, **Turolla, R.**, **Israel, G.L.**, **Zane, S.**, **Stella, L.**, **Mereghetti, S.**, **Tiengo, A.**, **Götz, D.**, **Göğüş, E. and Kouveliotou, C.**, 2010. A Low-Magnetic-Field Soft Gamma Repeater, *Science*, **330**, 944–, *1010.2781*.

[29] **Alpar, M.A.**, **Ertan, Ü. and Çalışkan, Ş.**, 2011. SGR 0418+5729-How does a Young Neutron Star Spin Down to a 9 s Period with a Dipole Field Less Than 10^{13} G?, *Astrophysical Journal Letters*, **732**, L4, *1102.1336*.

[30] **Bhattacharyya, S.**, 2010. X-ray views of neutron star low-mass X-ray binaries, *ArXiv e-prints*, *1002.4480*.

[31] **Chakrabarty, D.**, **Morgan, E.H.**, **Muno, M.P.**, **Galloway, D.K.**, **Wijnands, R.**, **van der Klis, M. and Markwardt, C.B.**, 2003. Nuclear-powered millisecond pulsars and the maximum spin frequency of neutron stars, *Nature*, **424**, 42–44, *arXiv:astro-ph/0307029*.

[32] **Patruno, A.**, 2010. Searching Sub-Millisecond Pulsars in Accreting Neutron Stars, *ArXiv e-prints*, *1007.1108*.

[33] **Markwardt, C.B. and Strohmayer, T.E.**, 2010. Discovery of Eclipses from the Accreting Millisecond X-ray Pulsar SWIFT J1749.4-2807, *Astrophysics Journal Letters*, **717**, L149–L153, *1005.3479*.

[34] **Markwardt, C.B.**, **Smith, E. and Swank, J.H.**, 2003. Discovery of a Fourth Accreting Millisecond Pulsar, XTE J1807-294, *The Astronomer's Telegram*, **122**, 1.

[35] **Heinke, C.O.**, **Altamirano, D.**, **Cohn, H.N.**, **Lugger, P.M.**, **Budac, S.A.**, **Servillat, M.**, **Linares, M.**, **Strohmayer, T.E.**, **Markwardt, C.B.**, **Wijnands, R.**, **Swank, J.H.**, **Knigge, C.**, **Bailyn, C. and Grindlay, J.E.**, 2010. Discovery of a Second Transient Low-Mass X-ray Binary in the Globular Cluster Ngc 6440, *Astrophysics Journal*, **714**, 894–903, *0911.0444*.

[36] **Galloway, D.K.**, **Markwardt, C.B.**, **Morgan, E.H.**, **Chakrabarty, D. and Strohmayer, T.E.**, 2005. Discovery of the Accretion-powered Millisecond X-Ray Pulsar IGR J00291+5934, *Astrophysics Journal Letters*, **622**, L45–L48, *arXiv:astro-ph/0501064*.

[37] **Markwardt, C.B. and Swank, J.H.**, 2003. XTE J1814-338, *IAU circular*, **8144**, 1.

[38] **Kaaret, P.**, **Morgan, E.H.**, **Vanderspek, R. and Tomsick, J.A.**, 2006. Discovery of the Millisecond X-Ray Pulsar HETE J1900.1-2455, *Astrophysics Journal*, **638**, 963–967, *arXiv:astro-ph/0510483*.

[39] **Markwardt, C.B.**, **Altamirano, D.**, **Swank, J.H.**, **Strohmayer, T.E.**, **Linares, M. and Pereira, D.**, 2009. RXTE Detects 245 Hz X-ray Pulsations from IGR J17511-305, *The Astronomer's Telegram*, **2197**, 1.

[40] **Markwardt, C.B.**, **Swank, J.H.**, **Strohmayer, T.E.**, **in 't Zand, J.J.M. and Marshall, F.E.**, 2002. Discovery of a Second Millisecond Accreting Pulsar: XTE J1751-305, *Astrophysics Journal Letters*, **575**, L21–L24, *arXiv:astro-ph/0206491*.

[41] **Altamirano, D.**, **Casella, P.**, **Patruno, A.**, **Wijnands, R. and van der Klis, M.**, 2008. Intermittent Millisecond X-Ray Pulsations from the Neutron Star X-Ray Transient SAX J1748.9-2021 in the Globular Cluster NGC 6440, *Astrophysics Journal Letters*, **674**, L45–L48, *0708.1316*.

[42] **Casella, P.**, **Altamirano, D.**, **Patruno, A.**, **Wijnands, R. and van der Klis, M.**, 2008. Discovery of Coherent Millisecond X-Ray Pulsations in Aquila X-1, *Astrophysics Journal Letters*, **674**, L41–L44, *0708.1110*.

[43] **Krimm, H.A.**, **Markwardt, C.B.**, **Deloye, C.J.**, **Romano, P.**, **Chakrabarty, D.**, **Campana, S.**, **Cummings, J.R.**, **Galloway, D.K.**, **Gehrels, N.**, **Hartman, J.M.**, **Kaaret, P.**, **Morgan, E.H. and Tueller, J.**, 2007. Discovery of the Accretion-powered Millisecond Pulsar SWIFT J1756.9-2508 with a Low-Mass Companion, *Astrophysics Journal Letters*, **668**, L147–L150.

[44] **Galloway, D.K.**, **Chakrabarty, D.**, **Morgan, E.H. and Remillard, R.A.**, 2002. Discovery of a High-Latitude Accreting Millisecond Pulsar in an Ultracompact Binary, *Astrophysics Journal Letters*, **576**, L137–L140, *arXiv:astro-ph/0206493*.

[45] **Galloway, D.K.**, **Muno, M.P.**, **Hartman, J.M.**, **Psaltis, D. and Chakrabarty, D.**, 2008. Thermonuclear (Type I) X-Ray Bursts Observed by the Rossi X-Ray Timing Explorer, *Astrophysical Journal Supplement Series*, **179**, 360–422, *arXiv:astro-ph/0608259*.

[46] **van der Klis, M.**, 1989. Quasi-periodic oscillations and noise in low-mass X-ray binaries, *Annual Reviews of Astronomy & Astrophysics*, **27**, 517–553.

[47] **Lamb, F.K.**, **Shibazaki, N.**, **Alpar, M.A. and Shaham, J.**, 1985. Quasi-periodic oscillations in bright galactic-bulge X-ray sources, *Nature*, **317**, 681–687.

[48] **Mitsuda, K.**, **Inoue, H.**, **Nakamura, N. and Tanaka, Y.**, 1989. Luminosity-related changes of the energy spectrum of X1608-522, *Publications of the Astronomical Society of Japan*, **41**, 97–111.

[49] **Done, C. and Gierliński, M.**, 2004. Spectral Transitions in X-Ray Binaries, *Progress of Theoretical Physics Supplement*, **155**, 9–18, *arXiv:astro-ph/0403546*.

[50] **Shakura, N.I. and Sunyaev, R.A.**, 1973. Black holes in binary systems. Observational appearance., *Astronomy and Astrophysics*, **24**, 337–355.

[51] **Narayan, R. and Yi, I.**, 1994. Advection-dominated accretion: A self-similar solution, *Astrophysics Journal Letters*, **428**, L13–L16, *arXiv:astro-ph/9403052*.

[52] **Esin, A.A.**, **McClintock, J.E. and Narayan, R.**, 1997. Advection-dominated Accretion and the Spectral States of Black Hole X-Ray Binaries: Application to Nova MUSCAE 1991, *Astrophysical Journal*, **489**, 865–+, *arXiv:astro-ph/9705237*.

[53] **Eggleton, P.P.**, 1983. Approximations to the radii of Roche lobes, *Astrophysics Journal*, **268**, 368.

[54] **Pringle, J.E.**, 1981. Accretion discs in astrophysics, *Annual Reviews of Astronomy and Astrophysics*, **19**, 137–162.

[55] **Ekşi, K.Y.**, **Hernquist, L. and Narayan, R.**, 2005. Where Are All the Fallback Disks? Constraints on Propeller Systems, *Astrophysical Journal Letters*, **623**, L41–L44, *arXiv:astro-ph/0501551*.

[56] **Ghosh, P. and Lamb, F.K.**, 1979. Accretion by rotating magnetic neutron stars. III - Accretion torques and period changes in pulsating X-ray sources, *Astrophysics Journal*, **234**, 296–316.

[57] **Narayan, R. and Yi, I.**, 1995. Advection-dominated Accretion: Underfed Black Holes and Neutron Stars, *Astrophysics Journal*, **452**, 710, *arXiv:astro-ph/9411059*.

[58] **Pringle, J.E. and Rees, M.J.**, 1972. Accretion Disc Models for Compact X-Ray Sources, *Astronomy and Astrophysics*, **21**, 1.

[59] **Ostriker, J.P. and Davidson, K.**, 1973. Models for Compact Pulsing X-Ray Sources, **H. Bradt & R. Giacconi**, editor, X- and Gamma-Ray Astronomy, volume 55 of *IAU Symposium*, p. 143.

[60] **Lamb, F.K.**, **Pethick, C.J. and Pines, D.**, 1973. A Model for Compact X-Ray Sources: Accretion by Rotating Magnetic Stars, *Astrophysics Journal*, **184**, 271–290.

[61] **Fabian, A.C. and Pringle, J.E.**, 1976. The importance of accretion torques in pulsing X-ray sources, *Monthly Notices of Royal Astronomical Society*, **174**, 25P–28P.

[62] **Wang, Y. and Robertson, J.A.**, 1985. 'Propeller' action by rotating neutron stars, *Astronomy and Astrophysics*, **151**, 361–371.

[63] **Zhang, S.N.**, **Yu, W. and Zhang, W.**, 1998. Spectral Transitions in Aquila X-1: Evidence for "Propeller" Effects, *Astrophysics Journal Letters*, **494**, L71, *arXiv:astro-ph/9711282*.

[64] **Campana, S.**, **Stella, L.**, **Mereghetti, S.**, **Colpi, M.**, **Tavani, M.**, **Ricci, D.**, **Fiume, D.D. and Belloni, T.**, 1998. Aquila X-1 from Outburst to Quiescence: The Onset of the Propeller Effect and Signs of a Turned-on Rotation-powered Pulsar, *Astrophysics Journal Letters*, **499**, L65, *arXiv:astro-ph/9803303*.

[65] **Rappaport, S.A.**, **Fregeau, J.M. and Spruit, H.**, 2004. Accretion onto Fast X-Ray Pulsars, *Astrophysical Journal*, **606**, 436–443, *arXiv:astro-ph/0310224*.

[66] **Riggio, A.**, **Burderi, L.**, **di Salvo, T.**, **Papitto, A.**, **D'Aì, A.**, **Iaria, R. and Menna, M.T.**, 2011. Secular spin-down of the AMP <ASTROBJ>XTE J1751-305</ASTROBJ>, *Astronomy and Astrophysics*, **531**, A140+, *1105.1984*.

[67] **Romanova, M.M.**, **Ustyugova, G.V.**, **Koldoba, A.V. and Lovelace, R.V.E.**, 2004. The Propeller Regime of Disk Accretion to a Rapidly Rotating Magnetized Star, *Astrophysical Journal*,, **616**, L151–L154, *arXiv:astro-ph/0502266*.

[68] **Romanova, M.M.**, **Ustyugova, G.V.**, **Koldoba, A.V. and Lovelace, R.V.E.**, 2005. Propeller-driven Outflows and Disk Oscillations, *Astrophysical Journal*, **635**, L165–L168, *arXiv:astro-ph/0511600*.

[69] **Michel, F.C. and Li, H.**, 1999. Electrodynamics of neutron stars, *Physics Reports*, **318**, 227–297.

[70] **Campana, S. and Stella, L.**, 2003. New results on neutron star low mass transients in the quiescence, *ArXiv Astrophysics e-prints*, *arXiv:astro-ph/0309811*.

CURRICULUM VITAE

Candidate's Full Name	**:**	Erlin KUTLU
Place and date of birth	**:**	İstanbul, 21/09/1975.
Permanent address	**:**	Karaoğlanoğlu Cad. No:38/6, Bahçelievler, İstanbul.
Universities and colleges attended	**:**	İstanbul Technical University, B.S in Physics Engineering , 1999. İstanbul University, Non-Thesis Master Programme Secondary School Physics Teacher , 2006.